Published in final edited form as:
Virus Res. 2012 July ; 167(1): 26–33. doi:10.1016/j.virusres.2012.03.015.

Sindbis Virus Infectivity Improves During the Course of Infection in Both Mammalian and Mosquito Cells

Kevin J. Sokoloski[A], **Chelsea A. Hayes**[A], **Megan P. Dunn**[B], **Jennifer L. Balke**[A], **Richard W. Hardy**[A,*], and **Suchetana Mukhopadhyay**[A,*]

[A]Department of Biology, Indiana University, 212 S. Hawthorne Drive, Bloomington, Indiana, 47405

Abstract

Alphaviruses are enveloped, single-stranded positive sense RNA viruses that are transmitted by an arthropod vector to a wide host range, including avian and mammalian species. Arthropods and vertebrates have different cellular environments and this may cause the different cellular pathologies that are observed between the invertebrate vector and vertebrate hosts in both whole organisms and cultured cell lines. In this report, we used Sindbis virus and examined mosquito and mammalian cell lines for their ability to produce progeny virus particles. Total particles produced, viral titers, and overall infectivity (or the ratio of total particles-to-infectious particles) was investigated. Our results show (1) Sindbis infectivity is more a function of the host cell used in titering the virus rather than the cell line used to produce the virus, (2) the number of total and infectious particles produced is cell line dependent, and (3) the infectivity of released virus particles improves during the course of infection in both cells that have cytolytic infections and persistent infections.

Keywords

Alphavirus; Sindbis; Particle formation; Infectivity assay; Host range; Virus spread

1. Introduction

Alphaviruses are enveloped, positive sense RNA viruses that are geographically diverse and are of particular concern to both human and livestock mammals. Alphaviruses are maintained in the environment via cyclical transmission between mammalian and avian hosts and vector mosquito species (Strauss and Strauss, 1994). This cyclical pattern of transmission is advantageous for the virus and leads to increased viral fitness (Weaver et al., 1999). While the importance of viral transmission between the mammalian host and vector mosquito is known, how virus infectivity, specifically particle formation and viral titer, is affected as a result of the cycle is less understood.

*Corresponding authors. Phone: (812) 856-0652 (RWH), (812)-856-3686 (SM). Fax: (812) 856-5710 (RWH, SM). rwhardy@indiana.edu (RWH), sumukhop@indiana.edu (SM).
[B]Current address: Franklin College, Department of Biology, 101 Branigin Blvd., Franklin, IN 46131

Alphavirus infection results in different outcomes depending on whether the host is a mammal or mosquito. These differences have been observed both in whole organisms and cell culture systems, primarily using Sindbis virus (SINV). Infection of a mammalian host leads to activation of a multitude of host cell responses including shutoff of host macromolecular synthesis at the levels of transcription and translation (Garmashova et al., 2007a; Garmashova et al., 2007b; Gorchakov, Frolova, and Frolov, 2005). Alphaviral infection in turn results in an acute cytolytic infection in mammalian cells. In culture using BHK-21, CHO, and 293HEK cells, cell death is evident within 24 hours post-infection. In contrast, infection of the mosquito results in the establishment of a persistent, infection lasting the life of the mosquito vector (Mims, Day, and Marshall, 1966). Moreover, host cell shutoff of transcription and translation is not observed in the majority of mosquito tissues, and in the commonly used cell lines, such as the *Aedes albopictus* C6/36 and *Aedes aegypti* Aag2, no cytopathic effect is observed (Raghow et al., 1973; Stollar et al., 1975; Stollar and Thomas, 1975; Tooker and Kennedy, 1981). Only in one reported mosquito cell line, the *Aedes albopictus* C7/10 cell line, has cell death been observed (Bowers, Coleman, and Brown, 2003; Karpf, Blake, and Brown, 1997; Sarver and Stollar, 1977).

The primary goal of these studies was to determine how SINV particle infectivity correlated with the cell type from which the SINV particle was derived. While the above differences between mammals and mosquitoes are widely accepted, the efficiency by which SINV is produced and the infectivity of these particles across other cell lines is less understood. The cellular environment of cultured mammalian and mosquito cells are different. The host factors that mediate virus replication and particle formation differ and studies are underway to determine the required host factors. Characterization of the released SINV particles from these different cell lines has not been well studied. It is generally accepted that SINV infectivity may be influenced by technical variations, such as serum quality and cell senescence. This study specifically aims to minimize these factors. In this work, we directly examine the infectivity of SINV during the course of infection in two standard laboratory cell lines, BHK-21 and C6/36, a mammalian and a mosquito cell line, respectively. To do this, we determined total particles produced by measuring genome copies via qRT-PCR and used an mCherry expressing SINV to determine titer via fluorescence foci formation. We found that the infectivity of SINV varies depending on the recipient host or the cell line used for titering the virus. Secondly, the amount of infectious SINV particles and total SINV particles produced, and the rate at which these particles are produced, depend on the cell line from which the virus is derived. Lastly, we found that SINV infectivity is temporally dependent and improved as infection progresses.

2. Materials and Methods

2.1 Cell Culture Maintenance

BHK-21, CHO, 293HEK, C6/36, and C7/10 cells were maintained in MEM (Cellgro) supplemented with 10% FBS (Atlanta Biologicals), 1x Antibiotic-Antimycotic Solution (Cellgro), 1x Non-Essential Amino Acid (NEAA) solution (Cellgro) and additional L-Glutamine (Cellgro). HeLa cells were maintained in DMEM (Gibco) supplemented with 10% FBS, 1x Antibiotic-Antimycotic Solution and 1x NEAA solution. Aag2 cells were cultured in Schneider's Drosophila S2 Media (Gibco) supplemented with 10% FBS and 1x Antibiotic-Antimycotic Solution. To minimize variations in the data due to media preparation cell culture reagents were standardized by lot number and maintained constant throughout the study. All mammalian cells were cultured at 37°C and 5% CO_2. Mosquito cell cultures were kept under similar conditions the only exception being the temperature of incubation was 28°C.

2.2 SINV-mCherry/FMV2A Construction

The SINV-mCherry FMV2A construct used in these studies was assembled as follows. A fusion of the mCherry gene and the Foot and Mouth virus 2A protease (FMV2A), a 17-amino acid sequence sufficient for auto-proteolytic cleavage, was created using overlapping PCR. The resulting fragment, mCherry/FMV2A, was inserted into the SINV TE12 cDNA clone at the junction between the capsid protein and the E3 protein with a three-part overlapping PCR strategy. This process resulted in the formation of the SINV-mCherry/FMV2A infectious clone.

2.3 SINV-mCherry/FMV2A Production/Derivation

Infectious SINV RNAs were produced *in vitro* using the method described in (Garneau et al., 2008). A total of 10 μg of full length SINV was electroporated into BHK-21 cells using a single pulse (1.5kV/25mA/200 Ohms). The cultures were allowed to progress for 48 hours prior to removal of the SINV containing supernatant. The viral supernatants were clarified via centrifugation at 1000×*g* for 5 minutes prior to being aliquoted and stored at −80°C for later use.

SINVs derived from other cell lines were produced similarly to the above process with the primary exception being that the cells were infected at an MOI=1 with SINV produced in BHK-21 cells.

2.4 Single-step Growth Curve Assay

Tissue culture cells were infected with SINV-mCherry/FMV2A at an MOI=3 for 1 hour at room temperature in 1xPBS (Cellgro) supplemented with 1% FBS, under gentle agitation. The infection medium was removed and the monolayers were washed twice with 1xPBS prior to the addition of growth media and further incubation. At regular intervals aliquots were removed and subjected to 5 minutes of centrifugation at 1500×*g* prior to being frozen at −80°C. The cell cultures were supplemented with media to restore initial volume and allowed to incubate further. This process was repeated every 6 hours for a period of 30 hours. Cell death was noted in the mammalian cell lines after 24 hours of infection. The collected SINV samples were assayed for titer on BHK-21 cells using the Fluorescent Foci Forming Assay described below.

2.4 SINV Fluorescent Foci Forming Assays

SINV-mCherry/FMV2A was serially diluted in 1xPBS supplemented with 1% FBS. Aliquots were added to monolayers of BHK-21, CHO, 293HEK, HeLa, C6/36 and C7/10 cells. Following an adsorption period of one hour at 25°C while gently rocking, the monolayers were overlaid with 1xMEM supplemented with 10% FBS, 1x Antibiotic-Antimycotic Solution, 1x NEAA Solution and 2% methylcellulose (6400 mPa, Sigma). The assays were returned to their respective incubation conditions and allowed to incubate for either 24 or 48 hours until fluorescent foci were apparent. The monolayers were fixed with 10% Formaldehyde (w/v diluted in distilled water, EMD Biosciences) and incubated for a minimum of one hour. The overlay was removed and the monolayers were rinsed with water to remove residual methylcellulose. The monolayers were imaged with a Typhoon 9200 phosphorimager (Fluorescence acquisition/532 excitation laser/610bp30 emission filter/100um resolution). Images were analyzed with ImageJ using the particle count feature and later confirmed with microscopy. In our experience the mCherry foci remained fluorescent for several days post fixation, provided they were kept hydrated with PBS.

2.5 Reverse Transcription and qRT-PCR

After thawing on ice, 5 μl aliquots of SINV supernatant were transferred to PCR tubes containing 500ng of both SINV nsp1 and E2 reverse transcription primers (nsp1 5′-AACATGAACTGGGTGGTG-3′; E2 5′-ATTGACCTTCGCGGTCGGATTCAT-3′). The samples were heated to 94°C for two minutes prior to 70°C for five minutes. The samples were removed to ice and processed using the ImpromII Reverse Transcriptase (Promega) according to the manufacturer's instructions. The samples were then either used immediately in the qRT-PCR protocol described below or stored at −20°C for later use. Detection of the SINV nsp1 and E2 regions were performed as according to the SYBR Brilliant Green III Supermix instructions (Agilent) with the following primer sets: SINVnsp1F 5′-AAGGATCTCCGGACCGTA-3′, SINVnsp1R 5′-AACATGAACTGGGTGGTGTCGAAG-3′; SINVE2F 5′-TCAGATGCACCACTGGTCTCAACA-3′, SINVE2R 5′-ATTGACCTTCGCGGTCGGATTCAT-3′. All of the oligonucleotides used in this study were obtained from Integrated DNA Technologies.

A total of 2 μls of the cDNA prepared above was added per well of a 96-well plate. A mixture consisting of 1x Brilliant SYBR Green reagent and 250nM Forward and Reverse detection primers was added to each well for a final volume of 25 μls. The standard curve consisted of 2 μls of serially diluted SINV infectious cDNA representing the potential range of the samples to be assayed. For each independent biological replicate, all qRT-PCR measurements, using both the nsP1, and E2 primer pairs, were made in duplicate and all data sets included paired standard curves and negative/mock infected controls.

Accurate quantification of the SINV genomes relied on relating the Ct values associated with the individual virus aliquots described above to a known standard curve. Serial dilution of the calibration standard reveals linear detection of SINV genomes ranging from 10^4 to 10^{11} genomes per ml. Minor signals, exhibiting melting points different from the genuine product, were detected in negative control wells (samples taken from uninfected cells). Furthermore, mock infected samples exhibited detection values corresponding to 2.0×10^5 ($+/-1.7\times10^5$) genome equivalents, well below the values observed for infected samples.

2.6 Calculation of Genome Copy

The observed Ct values from the standard curve described above were plotted and the trend examined using an exponential regression. The Ct values associated with the individual SINV samples were then examined using the equation obtained from the standard curve to determine the number of genomes present within the qRT-PCR reaction. From these data we were able to make precise measurements of the number of SINV particles in a given sample.

By multiplying the observed genome number by the dilution factor of the sample gives the concentration of the sample as a measurement of genomes per ml.

2.7 Statistical Analysis

Typical mathematical means and standard deviations were calculated and reported for all numerical data presented in this study. The analysis of cell derivation-specific infectivity (as reported in Figure 4), used variable bootstrapping to ensure that all deviation (from titer assays and particle quantification) was accounted for.

3. Results

3.1 SINV-mCherry FMV2A Produces Fluorescent Foci Upon Infection

A hallmark of SINV infection in many tissue culture models, such as BHK-21 cells, is the rapid formation of cytopathic effect (CPE) which allows for quantification of titer via plaque assay. Readily visible plaques form shortly after infection in many mammalian cell lines. Nevertheless, the reliance on CPE formation restricts the use of mosquito tissue culture systems since, to date, only the *Aedes albopictus* C7/10 cell line (and its derivatives) has been formally shown to exhibit CPE (Bowers, Coleman, and Brown, 2003; Karpf, Blake, and Brown, 1997). Other mosquito cell lines, for instance the commonly used *Aedes albopictus* C6/36 and *Aedes aegypti* Aag2 cell lines, do not exhibit overt CPE or other outward signs of infection (Karpf, Blake, and Brown, 1997; Raghow, Davey, and Dalgarno, 1973; Raghow et al., 1973; Stollar et al., 1975; Tooker and Kennedy, 1981). The inability to plaque on mosquito cells (outside of the C7/10 cell line) has limited efforts in the field to directly examine the progression of SINV infection in many mosquito cell lines.

Focus forming assays do not rely on the formation of CPE or cell death. Rather, virus-infected cells are detected by an alternative mark of infection, such as fluorescent protein expression. We generated a SINV construct that expresses the fluorescent protein mCherry from the subgenomic RNA without the inclusion of a second subgenomic promoter. This virus, SINV-mCherry/FMV2A, is similar to a mutant virus reported previously (Thomas et al., 2003). The position of the mCherry fluorophore (Figure 1A) enables the release of the fluorophore into the cytoplasm of the infected host cell without disruption of structural protein expression or processing. The expression of the structural ORF produces the capsid protein; which is autoproteolytically cleaved from the polypeptide (Ryan and Drew, 1994; Ryan, King, and Thomas, 1991). Translation of the mCherry encoding region results in the production of the mCherry/FMV2A fluorophore which is then cleaved from the remaining structural proteins via the FMV2A protease; a single proline residue is left on the N-terminus of the E3 protein (Ryan, King, and Thomas, 1991). The remainder of the polyprotein is translocated into the ER and spike formation occurs as in wild-type virus. Characterization of the SINV-mCherry/FMV2A virus via a one-step growth curve revealed kinetics similar to that of wild-type SINV with the primary exception being a 1-log-unit reduction in titer (Figure 1B). Examination of SINV protein processing indicates similar patterns of protein expression between the SINV-mCherry/FMV2A strain and wild-type SINV (data not shown).

Infection by SINV-mCherry/FMV2A in both mammalian and mosquito tissue culture cells results in the formation of red fluorescent foci, in addition to CPE in mammalian cell lines. As shown in Figure 1C, titration and subsequent detection of SINV-mCherry/FMV2A infected cells using fluorescence imaging indicates that SINV-mCherry/FMV2A fluorescence is readily quantifiable. Following further incubation, the fluorescent foci progressed into conventional plaques, indicating that a measurement of Fluorescent Foci-forming Units per ml (FFU/ml) is synonymous with the well-established PFU per ml measurement. Unless noted as wild-type SINV, the abbreviation SINV herein will refer to the SINV-mCherry/FMV2A virus.

The FFU assay described above and the conventional plaque assay determine the amount of infectious particles released during infection. During the course of an infection, non-infectious particles are also released. In order to assess the total number of particles released from an infected cell over time, we used a qRT-PCR based strategy to quantify the number of SINV genome equivalent per ml. This method was developed to allow for the rapid detection of particles released into the media that may either be too low of a concentration to reasonably purify or, in the case of assembly mutants, potentially too fragile to survive

sedimentation. Similar assays have been used to examine other arbovirus systems (Lee et al., 2010; Zybert et al., 2008).

Importantly, the nsP1 and E2 regions, which are greater than 8000nt apart, were observed in roughly equivalent quantities indicating full length genomes were present in particles. Furthermore this data indicates that little to no subgenomic RNAs were present. Moreover, with our experimental conditions of low MOIs and lengths of virus-host cell incubation times, defective interfering particles are unlikely to be formed. Therefore, we assert that the detection of nsP1 and E2 to similar levels corresponds to intact genomic RNA in the viral particles. Furthermore, treatment of the samples with RNAse A to degrade unprotected RNAs resulted in a statistically insignificant reduction in the number of SINV genomes (data not shown). Furthermore, we were unable to detect negative sense RNAs. These findings lead us to conclude that the SINV RNAs detected via qRT-PCR were indeed encapsidated and enveloped and not the product of cell necrosis or apoptosis.

3.2 SINV Infectivity is a Function of the Recipient Host Cell

The interplay between SINV derivation and recipient host has been previously noted in organisms and tissue culture systems, where SINV derivation in mosquito cells gives an apparent advantage to re-infection of BHK-21 cells (Mims, Day, and Marshall, 1966). We wished to determine if SINV infectivity, or particle-to-FFU, was variable across several commonly used cell lines or if this variation was restricted to a few select cell lines. In the experiments presented here, we did not serially passage the virus amongst or between the natural hosts, but rather measured infectivity from a single round of infection in the cell lines used in this study.

Full-length SINV RNA was transfected into BHK-21 cells to generate a SINV stock. The titer of this stock (in FFU/ml) was determined on BHK-21, CHO, 293HEK, HeLa, C6/36 and Aag2 (the cell lines examined in this study) to determine a cell-specific titer. We then determined cell-specific infectivity using the following protocol. We infected BHK-21 cells with our original stock SINV at a BHK-21 cell specific MOI=3 and harvested 16 hours post-infection to produce $SINV^{BHK\text{-}21}$. At this MOI and time of harvest, the amount of defective interfering particles should be minimal. We determined how many total particles were in this $SINV^{BHK\text{-}21}$ using qRT-PCR. We titered $SINV^{BHK\text{-}21}$ on different cell lines to see how the titer of the $SINV^{BHK\text{-}21}$ stock (FFU/ml) varied depending on the cell line used to determine titer. The infectivity of $SINV^{BHK\text{-}21}$ was determined as a ratio of total particles-to-infectious particles. The infectivity was plotted as a function of titer (since the particle number was constant) to determine how infectivity varies with the cell line used for titering the virus. This was repeated by generating SINV from different cell lines, $SINV^{CHO}$, $SINV^{293HEK}$, $SINV^{HeLa}$, $SINV^{C6/36}$, and $SINV^{Aag2}$ and each stock was analyzed as described for $SINV^{BHK\text{-}21}$. If SINV infectivity is more dependent upon the cell line used to titer the virus than the cell line use to derive the virus, then when infectivity is plotted against titer all points would fall along a diagonal. Yet if SINV infectivity is in fact influenced more by the derivating cell line than the cell line used to determine viral titer, the plotted infectivity values would be clustered together. The infectivity of each virus stock is shown in Figure 2, where we are showing the results from representative preparations of $SINV^{BHK\text{-}21}$, $SINV^{CHO}$, $SINV^{293HEK}$, $SINV^{HeLa}$, $SINV^{C6/36}$, and $SINV^{Aag2}$. This experiment has been performed at a minimum of twice for each cell line and the infectivity trends are highly similar between all independent preparations.

SINV derived from $SINV^{BHK\text{-}21}$, $SINV^{CHO}$, $SINV^{293HEK}$, $SINV^{C6/36}$, and $SINV^{Aag2}$ had similar trends; $SINV^{HeLa}$ was consistently found outside of the trend and therefore its results will be discussed separately. Total particles produced ranged from 2×10^8 ($SINV^{BHK\text{-}21}$) to 2×10^9 ($SINV^{293HEK}$). All SINV stocks showed differences in titer depending on the cell line

used to determine titer. As a result, the infectivity of SINV stock is variable and ranges from ~360 ($SINV^{Aag2}$ infecting C6/36 and Aag2 cells) to ~10 ($SINV^{Aag2}$ infecting BHK-21 and CHO cells, and $SINV^{CHO}$ and $SINV^{C6/36}$ infecting BHK-21 cells). Interestingly, there was no direct relationship between SINV infectivity and cell line (as noted by the different order of symbols in Figure 2), suggesting a complex relationship between SINV stock and host cell that could involve both genome replication and particle assembly.

$SINV^{HeLa}$ produced significantly less particles, 4×10^7 genomes/ml, compared to the other SINV stocks, and the titer of $SINV^{HeLa}$ was not dependent on cell line as the titers cluster closely. The only exception to this was when $SINV^{HeLa}$ was titered on HeLa cells and the infectivity was in the 10^3–10^4 FFU/ml range, almost 2-logs lower than when $SINV^{HeLa}$ was titered on other cell lines. The results from infectivity of $SINV^{HeLa}$ suggest these particles are more dependent upon the derivating cell line and may indicate a replication or assembly defect in these particles.

3.3 Mammalian and Mosquito Cells Produce Different Quantities of Infectious and Non-Infectious SINV Particles Over Time

SINV cycles between a mosquito vector and a mammalian host in nature and this cyclic infection pattern is critical for the fitness of the virus (Weaver et al., 1999). We have determined that SINV infectivity differed depending on if SINV was infecting a mammalian or mosquito cell line (Figure 2). We next sought to characterize SINV infectivity during the course of an infection in both mammalian and mosquito cell lines. Defining the SINV particles produced during the course of an infection may provide insight into titer, dissemination and spread within a host.

BHK-21 and C6/36 cells were infected with SINV at a cell specific MOI=3 and at six hour intervals samples were taken, the displaced media replaced, and then each stock was titered on BHK-21 and C6/36 cells by FFU/ml determination. As expected, the titer of $SINV^{BHK\text{-}21}$ and $SINV^{C6/36}$ increased regularly during the period surveyed with the cell lines exhibiting titers within 1-log-unit of each other by 24 hours post infection when titered on either BHK-21 or C6/36 cells (consistent with what is observed in Figure 2 when comparing the black diamonds and the open squares in $SINV^{BHK\text{-}21}$ and $SINV^{C6/36}$). In contrast, the number of particles produced by each cell line was different over time with $SINV^{BHK\text{-}21}$ producing 5×10^{10} particles and $SINV^{C6/36}$ producing 8×10^8 particles at 24 hours; the differences in particle number over time were greater than the differences in titer. From the titer and particle data, we determined that both $SINV^{BHK\text{-}21}$ and $SINV^{C6/36}$ particles released at late time points are more infectious. Higher infectivity is a more infectious viral stock or a lower ratio of total particles-to-infectious particles. $SINV^{BHK\text{-}21}$ showed an increase in infectivity from a ratio of 245+/−44 to 27+/−17 total particles-to-infectious particles and $SINV^{C6/36}$ showed an increase from in infectivity from a ratio of 600+/−135 to 2+/−1 total particles-to-infectious particles, during the first 24 hours of infection. Both values at 24 hours post-infection are consistent with reported particle-to-pfu values (Hernandez et al., 2003; Knight et al., 2009) but the increase in infectivity over time and the degree of the increase, was not expected.

After 24 hours, significant CPE was observed in the mammalian cell lines, preventing further assaying. The mosquito cell line C6/36 had reached peak titer by 24 hours and posted only modest increases at 30 hours post infection (data not shown).

3.4 SINV Infectivity Increases as Infection Progresses in Multiple Cell Lines

The variability in infectivity over time and the difference in infectivity depending on which cell line was used to titer the virus sample were unpredicted. To determine if variability in

infectivity was a general phenomenon, we infected different mammalian and mosquito cell lines with SINV at cell line specific MOI=3. Following removal of unadsorbed SINV, samples were taken at 6 hour intervals. The infectivity was determined by performing FFU assays on BHK-21 cells and the number of particles was determined by qRT-PCR to quantify the number of genomes. We titered all samples on BHK-21 cells to account for the cell line influenced variability in titer (as shown in Figure 2).

As shown in Figure 4A, SINV titers increased with respect to time for all cell lines assayed but at different rates. All cell lines used in this study reported mean titers of ~8.9×10^8 +/ −3.3×10^8 FFU/ml at 24 hours post-infection and displayed similar growth kinetics. The number of SINV particles released also increased over the same time period for all cell lines; however, the rate at which particle production increased differed between the cell lines. $SINV^{BHK\text{-}21}$, $SINV^{CHO}$ and $SINV^{293HEK}$ cells all posted an approximate 4-log-unit increase in particle production over a period of 24hrs. In contrast, $SINV^{HeLa}$ and $SINV^{Aag2}$ cells exhibited approximately a 2-log-unit increase over the same period of time. Moreover, $SINV^{C6/36}$ demonstrated only a 1-log-unit increase over 24 hours.

As a result, SINV infectivity improved as infection progressed (as exhibited by a decrease of the infectivity value) regardless of the cell line from which SINV was produced (shown in Figure 4C). Notably, at 24hrs, $SINV^{CHO}$ and $SINV^{Aag2}$ cells demonstrated infectivity values with an average of approximately 200:1 total particles-to-infectious particles, $SINV^{BHK\text{-}21}$, $SINV^{293HEK}$ and $SINV^{HeLa}$ exhibited average infectivity values on average of 40:1, while $SINV^{C6/36}$ showed the highest infectivity after 24 hours with a ratio of less than 5:1. The high infectivity of $SINV^{C6/36}$ is consistent with previous reports (Hernandez et al., 2003). To conclude, these data indicate that SINV infectivity is temporally dynamic and cell line specific.

4. Discussion

The primary goal of this study was to characterize how SINV particles varied over the course of an infection in commonly used lab cell culture systems. Using a qRT-PCR based assay in conjunction with a SINV that expresses a fluorescent protein, we were able to accurately and rapidly determine SINV infectivity, or ratio of total particle particles-to-infectious particles. The contributions of this study to our understanding of SINV biology are three-fold. First, this study represents a comprehensive examination of the relationship between SINV particle number and titer indicates that SINV infectivity is influenced by the host cell used to determine virus titer. Second this study indicates that not only do different cell lines produce a range of total particles, the efficiency by which these particles are produced varies. Finally, the infectivity of SINV is temporally dependent and improves as infection progresses independent of cell type.

The findings presented in Figure 2 suggest that SINV infectivity varies depending primarily on the host cell line. Since identical SINV stocks were used, particle number was independent of the host cell line and the differences observed in infectivity must be due to variations in SINV titer. This infers that the titer observed with a specific cell line is not universally applicable to other cell lines. These results suggest that titer, and hence MOI, should be determined within each individual cell line independently. One could envision two possible scenarios whereby the variation of infectivity could alter the outcome of the experiment. First, if an infection inadvertently used fewer infectious units than intended, an asynchronous infection and a mixed population of infected and uninfected cells would result. Second, if too many infectious units were applied, the formation of defective-interfering particles could result, or other aspects of the host response may be exacerbated. While the effects of either of the above scenarios are likely to be very complex, at the very

least the magnitudes of observed effects may be modulated. These findings potentially explain why a higher MOI may be needed with different viruses to achieve similar effects. Ignoring these variations has the potential to influence or confound the results of studies that rely on either synchronous infection or a precise correlation to dosage. This in turn may result in mixed populations of cells whereby biological effects may be masked, or minimized. These findings are likely not limited to arbovirology, but are further indications of viral biology as a whole.

The infectivity of SINV clearly improves as infection progresses and the ratio of total particles-to-infectious particles is time dependent. This implies that SINV samples taken at earlier stages of infection may contain significantly more particles than infectivity indicates. Moreover, assembly defects may be present early during infection, and at later stages (perhaps into persistence), particle assembly is increasingly accurate. For instance, comparing titer between different stages of infection may not be solely indicative of the progression of viral infection, as the samples have different compositions. Additionally, one could envision that SINV taken from the earlier stages of infection being more immunogenic or having a different immunogenicity as compared to those at later stages when the number of non-infectious particles produced has decreased.

Interestingly, improvement of SINV infectivity was largely reliant on the rate of particle production and not because of increases in titer. All the cell lines tested exhibited more or less equivalent growth kinetics (data not shown) but SINV particle production, however, varied temporally. In mammalian cells, SINV infection results in the shutoff of host macromolecular synthesis. As a result, one could speculate that the host cell environment becomes increasingly permissive to particle production and the viral synthesis machinery is more efficient, explaining the increased infectivity of SINV derived from mammalian cells. Nevertheless, the mosquito cell lines used in this study do not exhibit host cell translational shut off and these cells also display increases in particle production. Furthermore, the $SINV^{C6/36}$ particles had the greatest efficiency, via the smallest increase in particle production. The increased efficiency of $SINV^{C6/36}$ particles may be either a function of, or a cause of, alphaviral persistence in mosquito cells. Producing fewer particles, which are increasingly infectious, could be influential on the long term transmissibility of the viral infection.

Currently the precise mechanisms leading to increased SINV efficiency is unclear. A reasonable explanation is that the particles formed early during infection are somehow aberrant. At early stages of infection it is possible that core assembly and glycoprotein maturation are asynchronous. An accumulation of cytoplasmic nucleocapsid cores could result in premature budding and particle release. These particles would then exhibit limited infectivity compared to those produced at later times. Regardless, further understanding the events leading to the improvement of SINV infectivity would increase our understanding of Alphavirus biology.

Acknowledgments

The authors would like to thank the members of the Danthi, Hardy, and Mukhopadhyay labs for their efforts in development and implementation of this work. This work was supported by grant R01 AI0090077 from the NIAID/NIH to RWH.

References

Bowers DF, Coleman CG, Brown DT. Sindbis virus- associated pathology in Aedes albopictus (Diptera: Culicidae). J Med Entomol. 2003; 40(5):698–705. [PubMed: 14596286]

Garmashova N, Atasheva S, Kang W, Weaver SC, Frolova E, Frolov I. Analysis of Venezuelan equine encephalitis virus capsid protein function in the inhibition of cellular transcription. J Virol. 2007a; 81(24):13552–65. [PubMed: 17913819]

Garmashova N, Gorchakov R, Volkova E, Paessler S, Frolova E, Frolov I. The Old World and New World alphaviruses use different virus-specific proteins for induction of transcriptional shutoff. J Virol. 2007b; 81(5):2472–84. [PubMed: 17108023]

Garneau NL, Sokoloski KJ, Opyrchal M, Neff CP, Wilusz CJ, Wilusz J. The 3′ untranslated region of sindbis virus represses deadenylation of viral transcripts in mosquito and Mammalian cells. J Virol. 2008; 82 (2):880–92. [PubMed: 17977976]

Gorchakov R, Frolova E, Frolov I. Inhibition of transcription and translation in Sindbis virus-infected cells. J Virol. 2005; 79(15):9397–409. [PubMed: 16014903]

Hernandez R, Sinodis C, Horton M, Ferreira D, Yang C, Brown DT. Deletions in the transmembrane domain of a sindbis virus glycoprotein alter virus infectivity, stability, and host range. J Virol. 2003; 77(23):12710–9. [PubMed: 14610193]

Karpf AR, Blake JM, Brown DT. Characterization of the infection of Aedes albopictus cell clones by Sindbis virus. Virus Res. 1997; 50(1):1–13. [PubMed: 9255930]

Knight RL, Schultz KL, Kent RJ, Venkatesan M, Griffin DE. Role of N-linked glycosylation for sindbis virus infection and replication in vertebrate and invertebrate systems. J Virol. 2009; 83(11): 5640–7. [PubMed: 19297464]

Lee E, Leang SK, Davidson A, Lobigs M. Both E protein glycans adversely affect dengue virus infectivity but are beneficial for virion release. J Virol. 2010; 84(10):5171–80. [PubMed: 20219924]

Mims CA, Day MF, Marshall ID. Cytopathic effect of Semliki Forest virus in the mosquito Aedes aegypti. Am J Trop Med Hyg. 1966; 15(5):775–84. [PubMed: 5917634]

Raghow RS, Davey MW, Dalgarno L. The growth of Semliki Forest virus in cultured mosquito cells: ultrastructural observations. Arch Gesamte Virusforsch. 1973; 43(1):165–8. [PubMed: 4793529]

Raghow RS, Grace TD, Filshie BK, Bartley W, Dalgarno L. Ross River virus replication in cultured mosquito and mammalian cells: virus growth and correlated ultrastructural changes. J Gen Virol. 1973; 21:109–22. [PubMed: 4357368]

Ryan MD, Drew J. Foot-and-mouth disease virus 2A oligopeptide mediated cleavage of an artificial polyprotein. EMBO J. 1994; 13(4):928–33. [PubMed: 8112307]

Ryan MD, King AM, Thomas GP. Cleavage of foot-and-mouth disease virus polyprotein is mediated by residues located within a 19 amino acid sequence. J Gen Virol. 1991; 72 (Pt 11):2727–32. [PubMed: 1658199]

Sarver N, Stollar V. Sindbis virus-induced cytopathic effect in clones of Aedes albopictus (Singh) cells. Virology. 1977; 80(2):390–400. [PubMed: 196393]

Stollar V, Shenk TE, Koo R, Igarashi A, Schlesinger RW. Observations of Aedes albopictus cell cultures persistently infected with Sindbis virus. Ann N Y Acad Sci. 1975; 266:214–31. [PubMed: 1072595]

Stollar V, Thomas VL. An agent in the Aedes aegypti cell line (Peleg) which causes fusion of Aedes albopictus cells. Virology. 1975; 64(2):367–77. [PubMed: 806166]

Strauss JH, Strauss EG. The alphaviruses: gene expression, replication, and evolution. Microbiol Rev. 1994; 58(3):491–562. [PubMed: 7968923]

Thomas JM, Klimstra WB, Ryman KD, Heidner HW. Sindbis virus vectors designed to express a foreign protein as a cleavable component of the viral structural polyprotein. J Virol. 2003; 77(10): 5598–606. [PubMed: 12719552]

Tooker P, Kennedy SI. Semliki Forest virus multiplication in clones of Aedes albopictus cells. J Virol. 1981; 37(2):589–600. [PubMed: 7218433]

Weaver SC, Brault AC, Kang W, Holland JJ. Genetic and fitness changes accompanying adaptation of an arbovirus to vertebrate and invertebrate cells. J Virol. 1999; 73(5):4316–26. [PubMed: 10196330]

Zybert IA, van der Ende-Metselaar H, Wilschut J, Smit JM. Functional importance of dengue virus maturation: infectious properties of immature virions. J Gen Virol. 2008; 89(Pt 12):3047–51. [PubMed: 19008392]

- The cell line used to produce the Sindbis plays a minimal role in Sindbis infectivity
- The number of total and infectious particles produced is cell line dependent
- The infectivity of virus particles improves during the course of infection in six cell lines tested

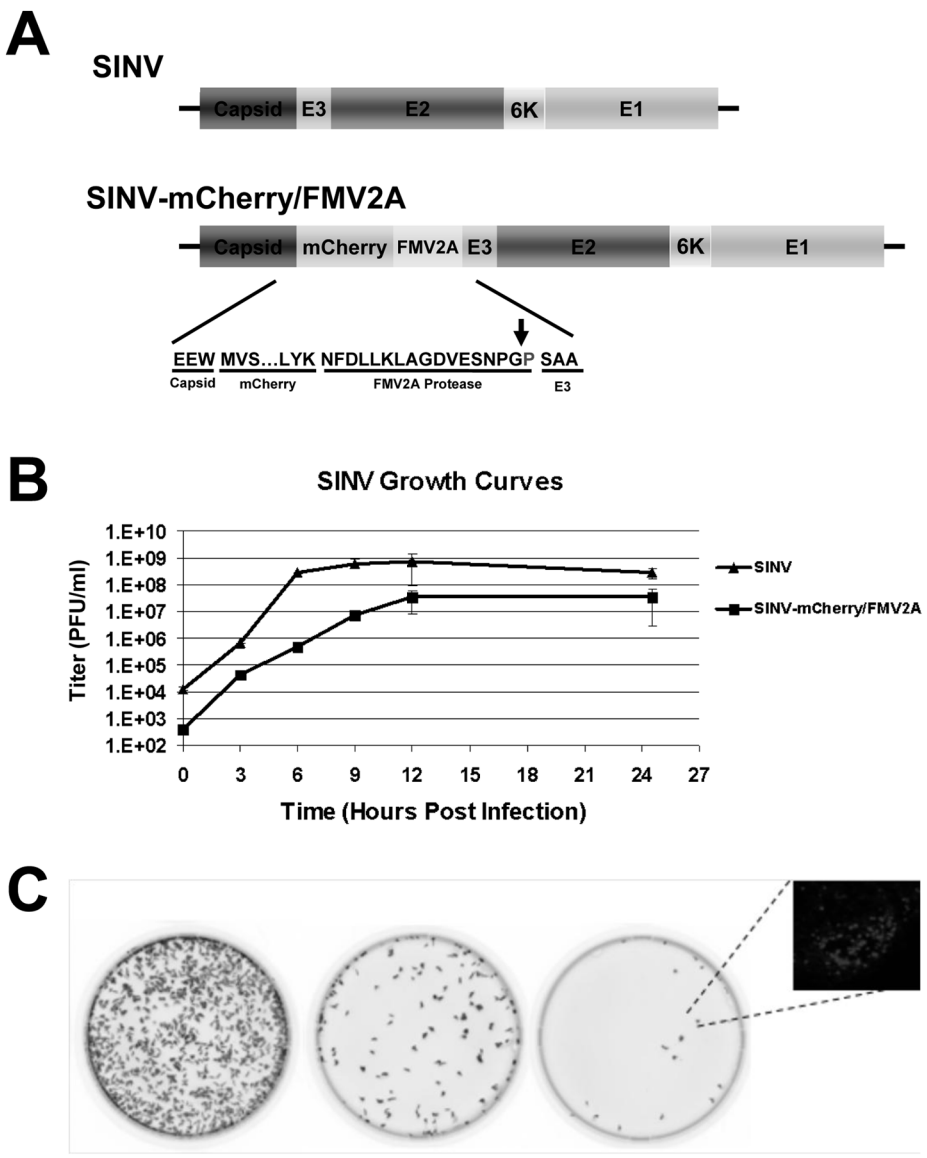

Figure 1. SINV-mCherry/FMV2A Produces Fluorescent Foci Upon Infection of Tissue Culture Cells

A) Schematic of the structural ORF of wild-type SINV and SINV-mCherry/FMV2A. Inset is the primary amino acid sequence of the cleavage site of the FMV2A protease and the arrow indicates the site of cleavage. **B)** Single-step growth curve of SINV-mCherry/FMV2A and wild-type SINV derived from BHK-21 cells and titered on BHK cells. Error bars indicate the standard deviation of three independent replicates. **C)** Phosphorimager scans of confluent BHK-21 monolayers infected with 10-fold dilutions of SINV-mCherry/FMV2A. Inset is a fluorescent microscopy image of a representative BHK-21 fluorescent focus at 24 hours post infection under 40x magnification.

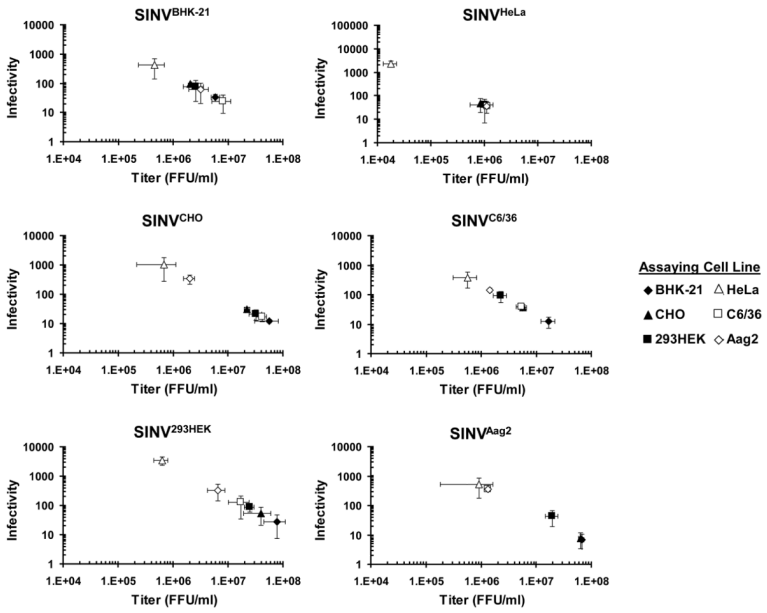

Figure 2. The Recipient Host Influences SINV Infectivity

A) Graphical representation of SINV infectivity versus titer. SINV stocks were generated from different cell lines, $SINV^{BHK\text{-}21}$, $SINV^{CHO}$, $SINV^{293HEK}$, $SINV^{HeLa}$, $SINV^{C6/36}$, and $SINV^{Aag2}$, and the particle concentration was determined. Each SINV stock was titered on six different cell lines to determine FFU/ml. The infectivity (total particles/infectious particles) was plotted as a function of titer. Values plotted are representative of two independent biological replicates. The plotted values are the means of two technical replicates and the error bars indicate the standard deviation.

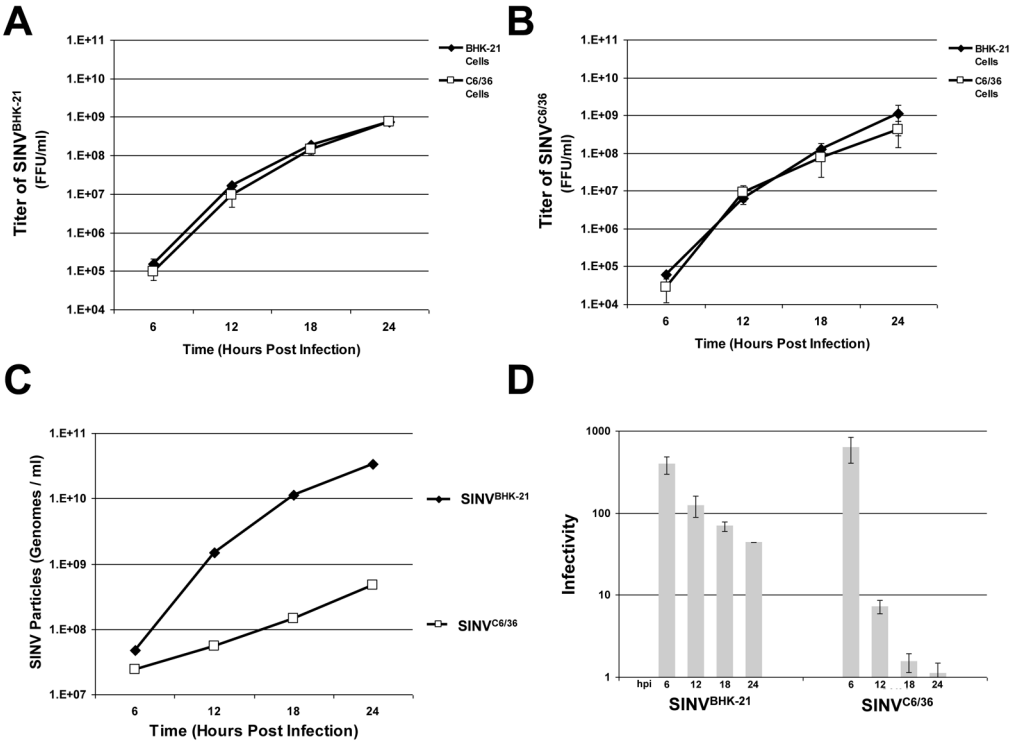

Figure 3. SINV Particle Production is Different Between Mammalian and Mosquito Cells

A) BHK-21 cells were infected with SINV at an MOI=3 and viral growth kinetics were observed at 6 hour intervals for 24 hours following infection. Values plotted are the titer of $SINV^{BHK-21}$ observed at each time point when assayed on BHK-21 or C6/36 cells. Values plotted are the averages of a minimum of two biological replicates, with error bars representing the standard deviation of four independent measurements. **B)** Identical to panel A, with the exception that SINV was produced in C6/36 cells ($SINV^{C6/36}$) instead of BHK-21 cells. **C)** Graphical representation of the number of $SINV^{BHK-21}$ and $SINV^{C6/36}$ particles produced during infection at the indicated time points. qRT-PCR was used to determine genome copies per ml. **D)** A bar graph illustrating the infectivity of $SINV^{BHK-21}$ and $SINV^{C6/36}$ over time. Values are the averages observed on both BHK-21 and C6/36 cells, with error bars representing the standard deviation.

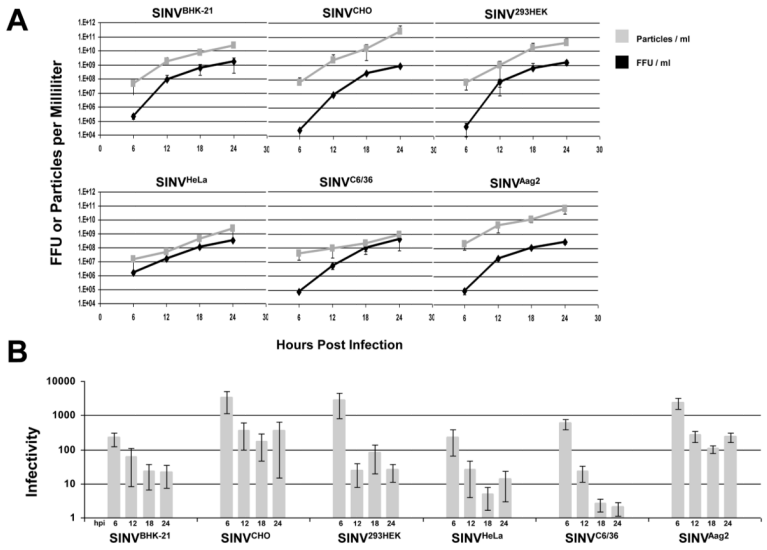

Figure 4. SINV Infectivity Increases as Infection Progresses

A) SINV virus was derived from different cell lines and graphs representing the number of SINV particles and infectious particles produced observed over time. **B)** Graphical representation of the SINV infectivity as observed in BHK-21 cells. Values plotted are the averages of two biological replicates, with error bars representing the standard deviation as determined by variable bootstrapping of four independent measurements of two independent preps.